Time-resolved, gas-phase kinetic and quantum chemical studies of the reaction of germylene with hydrogen chloride

Becerra, R., Cannady, J. P. and Walsh, R. ORCID: https://orcid.org/0000-0002-5096-6191 (2023) Time-resolved, gas-phase kinetic and quantum chemical studies of the reaction of germylene with hydrogen chloride. ChemPhysChem, 24 (10). e202200902. ISSN 1439-7641 doi: 10.1002/cphc.202200902 Available at https://centaur.reading.ac.uk/111154/

ChemPhysChem

Research Article
doi.org/10.1002/cphc.202200902

Chemistry Europe
European Chemical Societies Publishing

www.chemphyschem.org

Time-resolved, Gas-phase Kinetic and Quantum Chemical Studies of the Reaction of Germylene with Hydrogen Chloride

Rosa Becerra,[a] J. Pat Cannady,[b] and Robin Walsh*[c]

Time-resolved studies of germylene, GeH_2, generated by laser flash photolysis of 3,4-dimethyl-1-germacyclopent-3-ene at 193 nm and monitored by laser absorption, have been carried out to obtain rate constants for its bimolecular reaction with HCl. The reaction was studied in the gas phase, mainly at a total pressure of 10 Torr (in SF_6 bath gas) at five temperatures in the range 295–558 K. Experiments at other pressures showed that these rate constants were unaffected by pressure. The second-order rate constants at 10 Torr (SF_6 bath gas) fitted the Arrhenius equation: $\log(k/\text{cm}^3\,\text{molecule}^{-1}\,\text{s}^{-1}) = (-12.06 \pm 0.14) + (2.58 \pm 1.03\ \text{kJ mol}^{-1})/RT\ln 10$ where the uncertainties are single standard deviations. Quantum chemical calculations at G4 level support a mechanism in which an initial weakly bound donor-acceptor complex is formed. This can then rearrange and decompose to give H_2 and HGeCl (chlorogermylene). The enthalpy barrier (36 kJ mol^{-1}) is too high to allow rearrangement of the complex to GeH_3Cl (chlorogermane).

Introduction

Over the past 30 years, there has been a continuing interest in the chemistry of the divalent state of group 14 elements, the carbene analogues or heavy carbenes.[1–6] This has been stimulated, in part, by the increasing abilities of synthetic chemists to create these species in a stable form at room temperature, using the steric protection of bulky substituents or electronic stabilisation provided by incorporation into, or coordination with, an N-heterocyclic ring.[7–11] Nevertheless there still remains a need to uncover further details of the behaviour of the smaller, more reactive heavy carbenes in order to establish a reactivity baseline. We have devoted some years to the measurement, by time-resolved means, of gas phase rate constants for reactions of smaller silylenes[12–15] and germylenes[5,14] including the prototype species silylene, SiH_2, and germylene, GeH_2, as well as to the calculation of potential energy surfaces for many of their reactions. Much of the work carried out so far has been summarized in our 2007 review.[14] Less is known about the behaviour of GeH_2 and so we report further studies in the present paper. As well as our investigations[12–32] other kinetic studies have been undertaken by the group of King and Lawrance[33–35] in the gas phase and also by the group of Leigh[36] in the liquid phase, mainly of organogermylenes, GeR_2 (R = Me, Ph). A recent study by the group of Kaiser[37] has reported on the generation and gas phase behaviour of methylgermylene. These investigations show that GeH_2 and GeR_2 typically undergo bond insertion reactions into Ge–H, Si–H and O–H bonds, π-type addition reactions across C=C and C≡C bonds and reaction with lone pair donor molecules such as ethers. The first stage in these reactions is often thought to be formation of an intermediate complex in which the germylene acts as a lone pair acceptor (or Lewis acid).[12–14] In one study, Leigh's group have directly detected a GeH_2-alkene π-complex.[38] In general, the emerging pattern of reactivity shows much similarity to that of SiH_2[12,13] although rates for GeH_2 are somewhat slower, and GeH_2 shows more selectivity in its reactions than SiH_2.

There is, as yet, no kinetic study of GeH_2 with a chloride. Since we have previously studied the reaction of $SiH_2 + HCl$.[39] we thought it would be of interest to carry out a similar study of $GeH_2 + HCl$. To assist with the elucidation of potential products and reaction pathways and to further the comparison with $SiH_2 + HCl$, we have also carried out quantum chemical calculations of the potential energy surface for the reaction of $GeH_2 + HCl$. There has been no previous study, either experimental or theoretical, of this reaction system.

---

[a] Dr. R. Becerra
Instituto de Quimica-Fisica 'Rocasolano'
C.S.I.C., C/Serrano 119
28006 Madrid, Spain
[b] Dr. J. P. Cannady
Dow Chemical Company
2030 Dow Center
Midland, MI-48674, USA
[c] Prof. R. Walsh
Department of Chemistry
University of Reading
Whiteknights, P.O. Box 224
Reading, RG6 6AD, UK
E-mail: r.walsh@reading.ac.uk

Supporting information for this article is available on the WWW under https://doi.org/10.1002/cphc.202200902

Experimental and Theoretical Section

Equipment, Chemicals and Method

Germylene kinetic studies have been carried out by the laser flash photolysis/laser absorption technique, details of which have been published previously.[16,19] Only essential and brief details are therefore included here. GeH_2 was produced by the 193 nm flash photolysis of 3,4-dimethyl-1-germacyclopent-3-ene (DMGCP) by use of a Lambda Physik (Coherent) Compex 100 exciplex laser. The major photochemical pathway (90%) has been previously established[15] as the following:

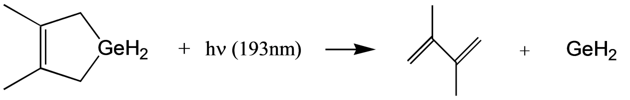

GeH_2 concentrations were monitored in real time (in absorption) by means of a Coherent 699–21 single-mode dye laser pumped by an Innova 90–5 Argon ion laser and operating with Rhodamine 6G. Experiments were carried out in a variable temperature spectrosil quartz vessel with demountable windows which were regularly cleaned. Photolysis laser pulse energies were typically 50–70 mJ with a variation of ±5%. The monitoring laser beam was multi-passed up to 40 times through the reaction zone to give an effective path length of up to 1.2 m. The laser wavelength was set by the combined use of a wavemeter (Burleigh WA-20) and reference to a known coincident transition in the visible spectrum of I_2 vapor and was checked at frequent intervals during the experiments.

The monitoring laser was tuned to 17111.31 cm^{-1} corresponding to a known strong vibration-rotation transition ($\tilde{A}^1B_1(0,1,0)\leftarrow\tilde{X}^1A_1(0,0,0)$ band) discovered by us originally.[16] Light signals were measured by a dual photodiode/differential amplifier combination and signal decays were stored in a transient recorder (Datalab DL 910) interfaced to a BBC microcomputer. This was used to average the decays of typically 5 laser shots (at a repetition rate of 0.5 or 1 Hz). Signals decays were found to be exponential up to 90% and were fitted by a least-squares procedure to provide values for the first order rate constants, k_{obs}, for removal of GeH_2 in the presence of known partial pressures of HCl. Examples of decays can be found in previous papers.[16,25]

The gas mixtures for photolysis were made up consisting of 0.4–1.5 mTorr of DMGCP, variable pressures of HCl between 0 and 9 Torr, and inert diluent bath gas, SF_6, up to total pressures between 1 and 100 Torr (although most experiments were performed at 10 Torr). Pressures were measured with capacitance manometers (MKS Baratron). All gases used in this work were frozen and rigorously pumped to remove any residual air prior to use. DMGCP was prepared as previously described.[16] HCl (99.9%) was from Aldrich. Sulfur hexafluoride, SF_6, (no GC-detectable impurities) was from Cambrian Gases.

Quantum Chemical (ab Initio) Calculations (Method)

The calculations reported here were done by the G4 method[40] using the Gaussian 16 package.[41] Transition state structures were characterised as first order saddle points by calculation of the hessian matrix. Stable structures, corresponding to energy minima, were identified by possessing no negative eigenvalues of the Hessian, whilst transition states were identified by having one and only one negative eigenvalue. The identities of the transition state structures were verified by calculation of Intrinsic Reaction Coordinates[42] (IRC). Reaction barriers were calculated as enthalpy differences at 298 K. Based on its extensive use for main group compounds,[43] we have found previously[44] that G4 gives reliable energy values for germanium compounds.

Results

Kinetic Measurements

It was independently verified during preliminary experiments that, for a given reaction mixture, k_{obs} values were not dependent on the exciplex laser energy or number of photolysis shots. Because static gas mixtures were used, tests with up to 10 shots were carried out. The constancy of k_{obs} (5 shot averages) showed no effective depletion of reactants. The sensitivity of detection of GeH_2 was high but decreased with increasing temperature: therefore increasing quantities of precursor were required at higher temperatures. However, at any given temperature precursor pressures were kept fixed to ensure a constant (but always small) contribution to k_{obs} values.

A series of experiments was carried out at five temperatures in the range 295–558 K: the highest temperature was limited by the thermal stability of the precursor. At each temperature and at total pressures of 10 Torr, a number of runs (at least five) at different HCl partial pressures was carried out. The results of these experiments are shown in Figure 1, which demonstrates the linear dependence of k_{obs} on [HCl], as expected for second-order kinetics. The non-zero intercepts correspond to reaction of GeH_2 with the precursor. The second order rate constants, k, obtained by least-squares fitting to these plots, are given in Table 1. The error limits are two standard deviations. An apparent anomaly that while the slopes of the plots in Figure 1 decrease monotonically with increasing temperature, the rate constants in Table 1 do not. This arises because the conversion from pressure to concentration is dependent on temperature. A few experiments at different total pressures up to 100 Torr (of added SF_6) were also carried out. In these experiments only one or two runs with different partial pressures of HCl were undertaken and second order kinetics was assumed. The rate constants from these experiments, also shown in Table 1, show

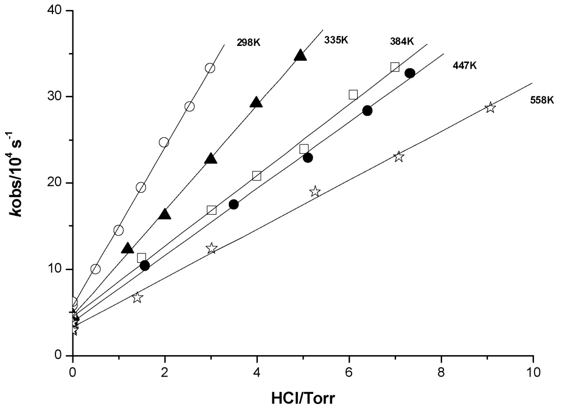

Figure 1. Second order plot for reaction of GeH_2 with HCl at various temperatures (indicated). Different symbols are used at each temperature.

Table 1. Experimental Second-Order Rate Constants for $GeH_2 + HCl$ at Several Temperatures and Total Pressures (in SF_6).

T/K P/Torr	$k/10^{-12}$ cm^3 molecule^{-1} s^{-1}[a] 10	 31	 100
298	2.84 ± 0.09	3.04	2.98
335	2.12 ± 0.05		
384	1.63 ± 0.07	1.88	1.85
447	1.78 ± 0.06	1.67	
558	1.64 ± 0.06	1.94	

[a] Uncertainties are 2 standard deviations.

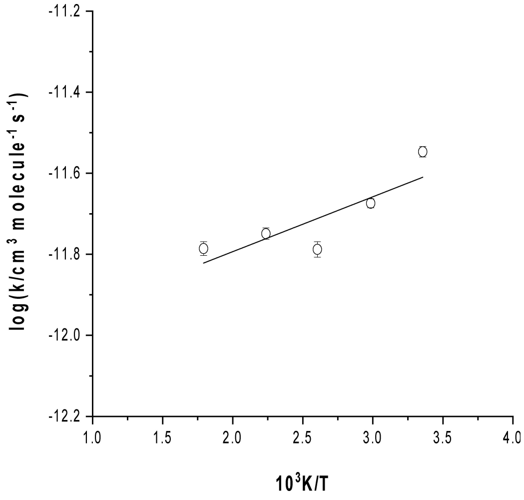

Figure 2. Arrhenius plot of rate coefficients for the reaction of GeH_2 with HCl.

small deviations from the 10 Torr values but no clearly defined pressure dependence. Despite some scatter, it is clear that the rate constants decrease with increasing temperature (just as has been found in other similar GeH_2 reactions[17–19,21–26]).

An Arrhenius plot of k (at 10 Torr) is shown in Figure 2. Since some of the points lie further from the best fit line than the scatter error bars indicate, this indicates that there must also be some systematic errors which we cannot quantify. A weighted least squares fit to the data correspond to the following equation:

$$\log(k/\mathrm{cm^3\,molecule^{-1}\,s^{-1}}) = (-12.06 \pm 0.14) + (2.58 \pm 1.03)\,\mathrm{kJ\,mol^{-1}}/RT\ \ln 10$$

where the uncertainties are single standard deviations.

Quantum Chemical (ab Initio) Calculations (Results)

Possible species on the GeH_3Cl potential energy surface (PES) were explored in some detail. A fairly straightforward energy profile and set of species has been found. The PES is shown in Figure 4 and Cartesian coordinates are given in the supporting information. Apart from the reactants, $GeH_2 + HCl$, this comprises three local minima (i.e. stable intermediates or products) and three transition states. The reaction pathway may be described as follows: the initial step to form a donor-acceptor complex (ylid), HCl···GeH_2 (in both *syn-* and *anti-* conformations), which, when it does not decompose back to reactants, can then either undergo an H-atom shift from Cl-to-Ge via transition state TS1 to form chlorogermane, GeH_3Cl^* (vibrationally excited) or decompose via TS2, a 4-centre process, to give hydrogen, H_2, and chlorogermylene, ClGeH. It is also potentially possible to reach $ClGeH + H_2$ by decomposition of GeH_3Cl (vibrationally excited) via TS3, a 3-centre process. Ignoring for the moment, the magnitudes of the TS barriers (see later discussion), this may be summarized in the following mechanistic scheme:

$$GeH_2 + HCl \rightarrow H_2Ge \cdots ClH$$

$$H_2Ge \cdots ClH \rightarrow GeH_3Cl^*$$

$$H_2Ge \cdots ClH \rightarrow HGeCl + H_2$$

$$GeH_3Cl^* \rightarrow HGeCl + H_2$$

$$GeH_3Cl^* + M \rightarrow GeH_3Cl$$

In this mechanism no distinction is made between the *syn-* and *anti-* forms of H_2Ge···ClH. Investigation of the energy profile between these two forms showed a low barrier of 0.3 kJ mol^{-1} which means almost free rotation around the Ge···Cl bond which connects the two forms. This also means that the IRC calculation which connects the complex to TS1 and TS2 cannot distinguish which form (conformer) connects to which transition state.

The structures of the intermediate species, products and reaction transition states are shown in Figure 3 and the enthalpy values are listed in Table 2 as well as being represented in Figure 4. In addition, we have calculated the enthalpies for the Cl- and H-atom transfer processes from HCl to GeH_2 to give the $ClGeH_2$ and GeH_3 radicals respectively. The enthalpies are relatively high and are only included in Table 2 for completeness, but the processes are not competitive and therefore not shown in Figure 4.

For comparison purposes we have included the energy values of a calculation using a simpler method (LPNO-CCSD(T).[45] These are shown in the supporting information.

Table 2. G4 Enthalpies for H_3GeCl Species of Interest in the Reaction of GeH_2 with HCl.

Species	H(298)/hartree	ΔH_{rel}/[kJmol^{-1}]
$GeH_2 + HCl$	−2538.325693	0
H_2Ge···ClH ylid-syn	−2538.334250	−22
H_2Ge···ClH ylid-anti	−2538.333903	−22
TS1	−2538.320313	+14
TS2	−2538.325856	0
H_3GeCl	−2538.40982	−221
TS3	−2538.322815	+8
$ClGeH + H_2$	−2538.368307	−112
$H_2GeCl + H$	−2538.276168	+130
$H_3Ge + Cl$	−2538.255471	+184

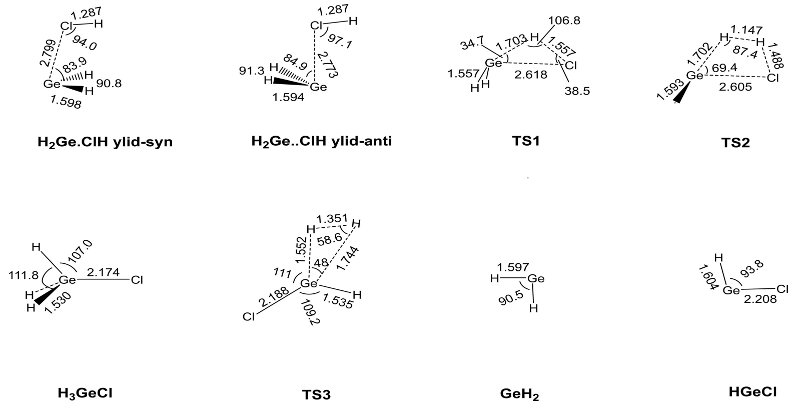

Figure 3. G4 calculated geometries of local minimum structures and transition states on the GeH_2+HCl energy surface. Selected distances are given in Å and angles in degrees.

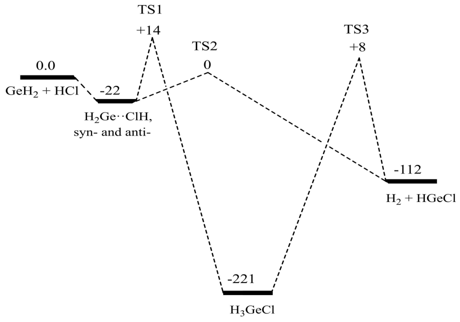

Figure 4. Potential energy (enthalpy) surface for the reaction of GeH_2+HCl at 298 K. All enthalpies ($kJ\,mol^{-1}$) are calculated at G4 level.

Discussion

General Comments and Rate Constant Comparisons

The main experimental purpose of this study was to measure the rate constants and their temperature dependence for the reaction of GeH_2 with HCl. This has been accomplished. There are no previous measurements of rate constants or Arrhenius parameters for this reaction. Some comparisons are, however, possible. Table 3 contains the rate constants for both GeH_2 and SiH_2 with HCl measured at similar temperatures[39] and shows clearly that SiH_2 is more reactive than GeH_2 by a factor of *ca* 2.5, a value which varies only slightly with temperature.

Table 3. Experimental Second-Order Rate Constants, k^a, for the Reactions of GeH_2 and SiH_2 with HCl at Similar Temperatures in SF_6 (10 Torr).

T/K	$k(GeH_2)$[a]	T/K	$k(SiH_2)$[a,b]	$k(SiH_2)/k(GeH_2)$
298	2.84 ± 0.09	296	7.23 ± 0.15	2.55 ± 0.16
335	2.12 ± 0.05	347	5.39 ± 0.20	2.54 ± 0.11
384	1.63 ± 0.07	411	5.34 ± 0.18	3.28 ± 0.18
447	1.78 ± 0.06	486	4.88 ± 0.18	2.74 ± 0.14
558	1.64 ± 0.06	611	4.66 ± 0.16	2.84 ± 0.14

[a] Units: $10^{-12}\,cm^3\,molecule^{-1}\,s^{-1}$ [b] Ref. [39].

To put this study into perspective, the Arrhenius parameters obtained here are compared with those of other germylene reactions,[18,21,24,26,32] as well as those of silylene reactions with the same substrates[39,46–49] in Table 4. Here it can be seen that this reaction possesses a similar small negative activation energy as other reactions of GeH_2, typical of a reaction proceeding via an association complex. The *A* factor is somewhat smaller than those of the other reactions in the table, indicating some possible steric hindrance in the reaction of GeH_2 with HCl. This may be illustrated further by consideration of Lennard-Jones collision efficiencies. These, and the collision numbers, Z_{LJ}, needed for their calculation, are given in Table 5. For the current reaction the value is 0.8% or 1 in 125. This is easily the lowest value of the reactions listed. It supports the idea that there is some special factor hindering the reaction. A

Table 4. Arrhenius Parameters for Prototype GeH_2 and SiH_2 Reactions.

Reaction	Log ($A/cm^3\,molecule^{-1}\,s^{-1}$)	$E_a/[kJ\,mol^{-1}]$	Ref.
GeH_2+GeH_4	-11.17 ± 0.10	-5.2 ± 0.7	18
GeH_2+SiH_4	-11.73 ± 0.06	-4.6 ± 0.42	21
$GeH_2+C_2H_4$	-10.61 ± 0.08	-5.4 ± 0.6	24
$GeH_2+C_2H_2$	-10.94 ± 0.05	-6.1 ± 0.4	26
GeH_2+SO_2	-11.01 ± 0.09	-4.6 ± 0.7	32
GeH_2+HCl	-12.06 ± 0.14	-2.6 ± 1.0	This work
SiH_2+SiH_4	-9.91 ± 0.04	-3.3 ± 0.3	45
$SiH_2+C_2H_4$	-9.97 ± 0.03	-2.9 ± 0.2	46
$SiH_2+C_2H_2$	-9.99 ± 0.03	-3.3 ± 0.2	47
SiH_2+SO_2	-10.10 ± 0.06	-3.5 ± 0.5	48
SiH_2+HCl	-11.51 ± 0.06	-1.9 ± 0.5	39

Table 5. Comparison of Lennard–Jones Collision Efficiencies for Reactions of GeH_2 with Selected Partners at 298 K.[a]

Reaction partner	K[b]	Z_{LJ}[b]	Efficiency/[%]
GeH_4	0.55	3.32	16.6
SiH_4	0.13	4.06	3.1
C_2H_4	2.10	4.40	48
C_2H_2	1.40	4.42	32
SO_2	0.668	3.60	19
HCl	0.028	3.53	0.80

[a] For references see Table 4. [b] Units: $10^{-10}\,cm^3\,molecule^{-1}\,s^{-1}$.

similarly low efficiency of 1.8% was found previously for the reaction of SiH_2 with HCl.[39] As discussed previously for SiH_2 reactions,[39] the efficient group of GeH_2 reactions includes bond insertion processes (GeH_4, SiH_4) and π-type additions (C_2H_4, C_2H_2). Reactions with O-donors (Me_2O, MeOH, CD_3OD and D_2O) are probably also in the efficient group, but the observed rate constants are pressure dependent[35] and, without modelling, their collisional (high-pressure) rate constants can only be approximately estimated.

The cause of this inefficiency of GeH_2+HCl can be understood when the potential energy surface is considered in more detail in the next section.

Quantum Chemical Calculations and Mechanism

Examination of Figure 4 indicates that both TS1 and TS3 have positive enthalpies. Unless these are in error, this shows that the reaction pathway cannot proceed via these channels. This leaves the route via TS2 as the only channel. With a predicted zero enthalpy barrier this is consistent with the small observed activation energy of $-2.6\ \mathrm{kJ\,mol^{-1}}$ within the uncertainty. It should be noted that while this true at G4 level, it would not be so for LPNO-CCD(T)[45] (TS2 has a predicted positive value; see supporting information).

We can use Transition State Theory (TST) to decide whether the G4 calculation is consistent with the observed Arrhenius *A* factor. For a second order rate constant, the TST expression[49] is $A=e^2(kT/h)\exp(\Delta S^{\ddagger}/R)$ where $\Delta S^{\ddagger}$ is the entropy of activation for TS2. The entropy values (in $\mathrm{J\,K^{-1}\,mol^{-1}}$, from the quantum chemical calculations) are 220.5 (GeH_2), 186.6 (HCl) and 277.5 (TS2) making $\Delta S^{\ddagger}=-129.6\ \mathrm{J\,K^{-1}\,mol^{-1}}$. This value becomes $-94.7\ \mathrm{J\,K^{-1}\,mol^{-1}}$ when converted from the standard state of 1 bar to that of $1\ \mathrm{mol\,dm^{-3}}$ (at 298 K).[49] This, in turn, gives $A(\mathrm{TST})=8.33\times10^{-13}\ \mathrm{cm^3\,molec^{-1}\,s^{-1}}$ and $\log[A(\mathrm{TST})/\mathrm{cm^3\,molec^{-1}\,s^{-1}}]=-12.08$. This is very close to the measured value (Table 4) and thus strongly supports the proposed mechanism via TS2. The reaction inefficiency may be attributed to the constraint of the 4-centred structure of TS2, required for molecular H_2 elimination. Because there is no energy barrier, this may be described as an entropy bottleneck. In the sequence of steps leading to TS2, the donor-acceptor complexes are almost certainly in equilibrium with the reactants, viz, they re-dissociate faster than rearrange via TS2. As long as formation of TS2 is the rate determining stage this is an inevitable consequence.

The possibility that the reaction inefficiency could have resulted from *overall* reversibility can be ruled out. We have calculated a value of 1.0×10^{19} for the equilibrium constant at 298 K for $GeH_2+HCl\leftrightarrows HGeCl+H_2$ (see supporting information).

This is far too high to permit any contribution from the back reaction, even at higher temperatures. The main contributing factor to this high value is the enthalpy release ($\Delta H=-112\ \mathrm{kJ\,mol^{-1}}$), giving the reverse reaction a significant barrier to overcome.

For comparison, the potential energy (enthalpy) surface for the reaction of SiH_2+HCl[39] is shown in Figure 5. The principal differences from Figure 4 are the relative heights of the barriers for TS1 and TS3. For SiH_2+HCl they both lie below the threshold, thus making these channels accessible. The consequence is that the association complex, $ClH\cdots SiH_2$ reacts, at least in part, to give SiH_3Cl^* as well as $ClSiH+H_2$, whereas for GeH_2+HCl, the complexes $HCl\cdots GeH_2$ only give $ClGeH+H_2$. For SiH_2+HCl, part of the yield of $ClSiH+H_2$ may also come via TS3, whereas for GeH_2+HCl it is only formed via TS2.

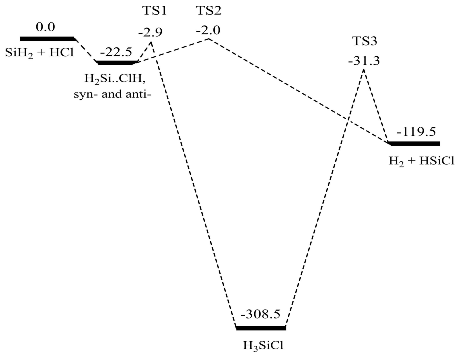

Figure 5. Potential energy (enthalpy) surface for the reaction of SiH_2+HCl at 298 K. All enthalpies ($\mathrm{kJ\,mol^{-1}}$) were calculated at G3 level.[39]

Probably the largest contributing factors to these differences are the increased lengths of the Ge–H and Ge–Cl bonds[44] compared with Si–H and Si–Cl bonds. These cause greater constriction of the geometries of the transition states TS1 and TS3 compared with their Si counterparts. Other factors which contribute to these differences are the reduced strengths of Ge–H and Ge–Cl bonds[44] compared with Si–H and Si–Cl bonds respectively.[51]

Conclusions

GeH_2 reacts with HCl in a simple reaction to form H_2 and HGeCl. Although it has no energy barrier the reaction occurs at less than 1% of collision efficiency. The cause of this inefficiency is revealed by quantum chemical calculations which indicate a transition state structure which provides an entropy bottleneck. This study extends the range of behaviour that GeH_2 shows in its reactions with small molecules.

Conflict of Interest

The authors declare no conflict of interest.

Data Availability Statement

The data that support the findings of this study are available in the supplementary material of this article.

Keywords: gas phase · germylene · hydrogen chloride · kinetics · laser flash photolysis

[1] W. P. Neumann, *Chem. Rev.* **1991**, *91*, 311–334.
[2] P. P. Gaspar, R. West, *Silylenes in The Chemistry of Organosilicon Compounds*, Z. Rappoport, Y. Apeloig, Eds.; Wiley; Chichester **1998**, Vol. 2, Chapter 43, p 2463.
[3] S. E. Boganov, M. P. Egorov, V. I. Faustov, O.M Nefedov, in *The Chemistry of Organic Germanium, Thin and Lead Compounds*; Rappoport, Z., Eds.; Wiley; Chichester **2002**, Vol. 2, part 1, p 749.
[4] N. Tokitoh, W. Ando, In *Reactive Intermediate Chemistry*, R. A. Moss, M. S. Platz, M. Jones, Jr., Eds.; Wiley & Sons, NY **2004**, Chapter 14, p. 651.
[5] S. E. Boganov, M. P. Egorov, V. I. Faustov, I. V. Krylova, O. M. Nefedov, R. Becerra, R. Walsh, *Russ. Chem. Bull. Int. Ed.* **2005**, *54*, 483–511.
[6] Y. V. Tomilov, L. G. Menchikov, E. A. Shapiro, V. D. Gvozdev, K. N. Shavrin, N. V. Volchkov, M. B. Lipkind, M. P. Egorov, S. E. Boganov, V. N. Khabashesku, E. G. Baskir, *Mendeleev Commun.* **2021**, *31*, 750–768.
[7] Y. Mizubhata, T. Sasamori, N. Tokitoh, *Chem. Rev.* **2009**, *109*, 3479–3511.
[8] M. Kira, *Dalton Trans.* **2010**, *39*, 9175–9175.
[9] V. Y. Lee, A. Sekiguchi, in *Organometallic compounds of low coordinate Si, Ge, Sn and Pb: from Phantom species to stable compounds* Wiley, Chichester **2010**, chapter 4, p. 139.
[10] S. G. Ghadwal, R. Azhakar, H. W. Roesky, *Acc. Chem. Res.* **2013**, *46*, 444–456.
[11] C. Shan, S. Yao, M. Driess, *Chem. Soc. Rev.* **2020**, *49*, 6733–6754.
[12] R. Becerra, R. Walsh, *Kinetics and mechanisms of silylene reactions: a prototype for gas-phase acid/base chemistry. In: Research in Chemical Kinetics*, eds R. G. Compton, G. Hancock, Elsevier, Amsterdam **1995**, vol. 3, chap. 6, p. 263.
[13] J. M. Jasinski, R. Becerra, R. Walsh, *Chem. Rev.* **1995**, *95*, 1203–1228.
[14] R. Becerra, R. Walsh, *Phys. Chem. Chem. Phys.* **2007**, *9*, 2817–2835.
[15] R. Becerra, R. Walsh, *Dalton Trans.* **2010**, *39*, 9217–9228 and references cited there.
[16] R. Becerra, S. E. Boganov, M. P. Egorov, O. M. Nefedov, R. Walsh, *Chem. Phys. Lett.* **1996**, *260*, 433–440.
[17] R. Becerra, S. E. Boganov, M. P. Egorov, O. M. Nefedov, R. Walsh, *Mendeleev Commun.* **1997**, 87–88.
[18] R. Becerra, S. E. Boganov, M. P. Egorov, V. I. Faustov, O. M. Nefedov, R. Walsh, *J. Am. Chem. Soc.* **1998**, *120*, 12657–12665.
[19] R. Becerra, R. Walsh, *Phys. Chem. Chem. Phys.* **1999**, *1*, 5301–5304.
[20] R. Becerra, S. E. Boganov, M. P. Egorov, V. I. Faustov, O. M. Nefedov, R. Walsh, *Can. J. Chem.* **2000**, *78*, 1428–1435.
[21] R. Becerra, S. E. Boganov, M. P. Egorov, V. I. Faustov, O. M. Nefedov, R. Walsh, *Phys. Chem. Chem. Phys.* **2001**, *3*, 184–192.
[22] R. Becerra, R. Walsh, *J. Organomet. Chem.* **2001**, *636*, 49–56.
[23] R. Becerra, M. P. Egorov, I. V. Krylova, O. M. Nefedov, R. Walsh, *Chem. Phys. Lett.* **2002**, *351*, 47–52.
[24] R. Becerra, S. E. Boganov, M. P. Egorov, V. I. Faustov, V. M. Promyslov, O. M. Nefedov, R. Walsh, *Phys. Chem. Chem. Phys.* **2002**, *4*, 5079–5087.
[25] R. Becerra, R. Walsh, *Phys. Chem. Chem. Phys.* **2002**, *4*, 6001–6005.
[26] R. Becerra, S. E. Boganov, M. P. Egorov, V. I. Faustov, I. V. Krylova, O. M. Nefedov, V. M. Promyslov, R. Walsh, *Phys. Chem. Chem. Phys.* **2004**, *6*, 3370–3382.
[27] R. Becerra, C. R, Harrington, W. J. Leigh, L. A. Kefala, R. Walsh, *Organometallics* **2006**, *25*, 4439–4443.
[28] R. Becerra, S. E. Boganov, M. P. Egorov, I. V. Krylova, O. M. Nefedov, R. Walsh, *J. Phys. Chem. A* **2007**, *111*, 1434–1440.
[29] R. Becerra, S. E. Boganov, M. P. Egorov, V. I. Faustov, I. V. Krylova, O. M. Nefedov, V. M. Promyslov, R. Walsh, *Phys. Chem. Chem. Phys.* **2007**, *9*, 4395–4406.
[30] R. Becerra, R. Walsh, *Phys. Chem. Chem. Phys.* **2009**, *11*, 3539–3546.
[31] R. Becerra, R. Walsh, *Phys. Chem. Chem. Phys.* **2010**, *12*, 2923–2928.
[32] R. Becerra, J. P. Cannady, R. Walsh, *Organometallics* **2014**, *33*, 6493–6503.
[33] U. N. Alexander, N. A. Trout, K. D. King, W. D. Lawrance, *Chem. Phys. Lett.* **1999**, *299*, 291–295.
[34] U. N. Alexander, K. D. King, W. D. Lawrance, *Chem. Phys. Lett.* **2000**, *319*, 529–534.
[35] U. N. Alexander, K. D. King, W. D. Lawrance, *Phys. Chem. Chem. Phys.* **2003**, *5*, 1557–1561.
[36] S. S. Kostina, W. J. Leigh, *Can. J. Chem.* **2015**, *9*, 435–444, and references cited therein.
[37] Z. Yang, Ch. He, S. Doddipatla, V. S. Krasnoukhov, V. N. Azyazov, A. M. Mebel, R. I. Kaiser, *ChemPhysChem* **2020**, *21*, 1898–1904.
[38] P. S. Billone, K. Beleznay, C. R. Harrington, L. A. Huck, W. J. Leigh, *J. Am. Chem. Soc.* **2011**, *133*, 10523–10534.
[39] R. Becerra, J. P. Cannady, R. Walsh, *J. Phys. Chem. A* **2004**, *108*, 3987–3993.
[40] L. A. Curtiss, P. C. Redfern, K. Raghavachari, *J. Chem. Phys.* **2007**, *126*, 084108–1–084108-12.
[41] Gaussian 16 (Revision B-01), M. J. Frisch, G. W. Trucks, H. B. Schlegel, G. E. Scuseria, M. A. Robb, J. R. Cheeseman, G. Scalmani, V. Barone, G. A. Petersson, H. Nakatsuji, X. Li, M. Caricato, A. V. Marenich, J. Bloino, B. G. Janesko, R.Gomperts, B. Mennucci, H. P. Hratchian, J. V. Ortiz, A. F. Izmaylov, J. L. Sonnenberg, D. Williams-Young, F. Ding, F. Lipparini, F. Egidi, J. Goings, B. Peng, A. Petrone, T. Henderson, D. Ranasinghe, V. G. Zakrzewski, J. Gao, N. Rega, G. Zheng, W. Liang, M. Hada, M. Ehara, K. Toyota, R. Fukuda, J. Hasegawa, M. Ishida, T. Nakajima, Y. Honda, O. Kitao, H. Nakai, T. Vreven, K. Throssell, J. A. Montgomery, Jr. J. E. Peralta, F. Ogliaro, M. J. Bearpark, J. J. Heyd, E. N. Brothers, K. N. Kudin, V. N. Staroverov, T. A. Keith, R. Kobayashi, J. Normand, K. Raghavachari, A. P. Rendell, J. C. Burant, S. S. Iyengar, J. Tomasi, M. Cossi, J. M. Millam, M. Klene, C. Adamo, R. Cammi, J. W. Ochterski, R. L. Martin, K. Morokuma, O. Farkas, J. B. Foresman, D. J. and Fox, Gaussian Inc., Wallingford CT **2016**.
[42] C. Gonzales, H. C. Schlegel, *J. Chem. Phys.* **1989**, *90*, 2154–2161.
[43] S. Rayne, K. Forest, *Comput. Theor. Chem.* **2011**, *974*, 163–179.
[44] R. Becerra, R. Walsh, *Phys. Chem. Chem. Phys.* **2019**, *21*, 988–1008.
[45] B. E. Krysyuk, T. M. Sypko, I. N. Zyuzin, *FirePhysChem* **2023**, in press.
[46] R. Becerra, H. M. Frey, B. P. Mason, R. Walsh, M. S. Gordon, *J. Chem. Soc. Faraday Trans.* **1995**, *91*, 2723–2732.
[47] N. Al-Rubaiey, R. Walsh, *J. Phys. Chem.* **1994**, *98*, 5303–5309.
[48] R. Becerra, J. P. Cannady, G. Dormer, R. Walsh, *J. Phys. Chem. A* **2008**, *112*, 8665–8677.
[49] R. Becerra, J. P. Cannady, N. Goldberg, R. Walsh, *Phys. Chem. Chem. Phys.* **2013**, *15*, 14748–14760.
[50] S. W. Benson, *Thermochemical Kinetics*, 2nd ed.; Wiley: New York **1976**.
[51] R. Becerra, R. Walsh, *Thermochemistry of Organosilicon Compounds. In Organosilicon Compounds*, Vladimir Ya Lee, Ed. Elsevier **2017**, Vol. 2, Chapter 3, p. 79.

Manuscript received: December 8, 2022
Revised manuscript received: February 15, 2023
Accepted manuscript online: February 21, 2023
Version of record online: ■■, ■■

RESEARCH ARTICLE

Kinetic measurements combined with quantum chemical theory show that this fast reaction proceeds solely via this pathway, with no GeH_3Cl intermediary.

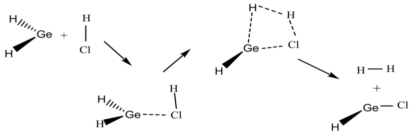

*Dr. R. Becerra, Dr. J. P. Cannady, Prof. R. Walsh**

1 – 7

Time-resolved, Gas-phase Kinetic and Quantum Chemical Studies of the Reaction of Germylene with Hydrogen Chloride